resulting antiferromagnetic alignment of unpaired spins from $d_{xy,xz}$–π–$d_{xy,xz}$ overlap must arise from secondary factors. Some unpaired spin density will be incorporated in the d_{xy} orbital allowing for a d_{xy}–$\pi(b_{2g})$–d_{xy} superexchange pathway.

In the $Cu(hfac)_2$·pyr complex the plane of the pyrazine ligands lies in the xz plane of the $Cu(hfac)_2$ unit.[4] The site symmetry about the copper(II) ion is C_{2h}. If superexchange is to occur by a π pathway, we need only consider overlap of the $d_{x^2-y^2}$, d_{xy}, and d_{z^2} orbitals of copper with the π system of pyrazine since under C_{2h} symmetry these are the only metal orbitals with unpaired spin density. The only symmetry-allowed overlap with the pyrazine π system arises from d_{xy}–$\pi(b_{1g})$ overlap corresponding to the $d_{x^2-y^2}$–$\pi(b_{1g})$ overlap in $Cu(NO_3)_2$·pyr (Figure 4a). However, in $Cu(hfac)_2$·pyr we have the combination of the small amount of unpaired spin density in d_{xy} and poor effective overlap as obtains from d–$\pi(b_{1g})$ orbitals. A superexchange interaction in $Cu(hfac)_2$·pyr was not observed within the limits of our experiments (1.8 K) even though a π pathway is available.

The magnetic susceptibility data as a function of temperature for the $Cu(hfac)_2$·Dabco complex do not reveal magnetic-exchange interactions. The only tenable pathway for superexchange along the chain is by way of σ orbitals, since Dabco is without a π system; however, exchange along a σ pathway would be severely attenuated over the long Cu–Cu separation of 7.7 Å.[11] Also, the metal orbital that overlaps with the σ system of the Dabco is mainly of d_{z^2} character, and this orbital has little unpaired spin density.

The $Cu(NO_3)_2$·nap complex[9] has been studied previously by magnetic susceptibility methods and found to exhibit enhanced spin coupling relative to the $Cu(NO_3)_2$·pyr complex in spite of the larger Cu–Cu separation (~9 Å vs. 6.7 Å). The enhanced spin coupling relative to pyrazine is a consequence of the nature of the π system of the 1,5-naphthyridine. Our initial interest in studying the complex $Cu(hfac)_2$·nap was stimulated by the greater basicity of 1,5-naphthyridine. We attempted to prepare a $Cu(hfac)_2$ complex with in-plane copper–nitrogen bonds analogous to *cis*-$Cu(hfac)_2$·2py.[29] We conjectured the possibility that the stability of the in-plane pyridine arrangement was due to the greater basicity of the pyridine ligand ($pK_a \approx 5.2$) as compared to that of pyrazine. A cis or trans arrangement for the $Cu(hfac)_2$·nap should have given rise to dimeric or polymeric structures, respectively, and the expected shorter (in-plane) copper–ligand bond should have been more conducive to magnetic-exchange interactions. The electronic, EPR, and magnetic data (see Table I) for the $Cu(hfac)_2$·nap complex are virtually analogous to the data for $Cu(hfac)_2$·pyr and $Cu(hfac)_2$·Dabco, and we conclude that its structure is similar.

Acknowledgment. This research was supported by the National Science Foundation under Grant No. MPS74-11495 and by the Materials Research Center of the University of North Carolina under Grant No. DMR72-03024 from the National Science Foundation.

Registry No. $Cu(hfac)_2$·pyr, 52151-41-4; $Cu(hfac)_2$·nap, 61075-79-4; $Cu(hfac)_2$·Dabco, 38548-37-7.

References and Notes

(1) J. F. Villa and W. E. Hatfield, *J. Am. Chem. Soc.*, **93**, 4081 (1971).
(2) D. B. Losee, H. W. Richardson, and W. E. Hatfield, *J. Chem. Phys.*, **59**, 3600 (1973).
(3) H. W. Richardson and W. E. Hatfield, *J. Am. Chem. Soc.*, **98**, 835 (1976).
(4) R. C. E. Belford, D. E. Fenton, and M. R. Truter, *J. Chem. Soc., Dalton Trans.*, 17 (1974).
(5) C. Creutz and H. Taube, *J. Am. Chem. Soc.*, **95**, 1006 (1973).
(6) R. W. Callahan, G. M. Brown, and T. J. Meyer, *Inorg. Chem.*, **14**, 1443 (1975).
(7) A. Chia and R. F. Trimble, Jr., *J. Phys. Chem.*, **65**, 863 (1961).
(8) H. W. Richardson, W. E. Hatfield, H. J. Stoklosa, and J. R. Wasson, *Inorg. Chem.*, **12**, 2051 (1973).
(9) H. J. Stoklosa, J. R. Wasson, E. V. Brown, H. W. Richardson, and W. E. Hatfield, *Inorg. Chem.*, **14**, 2378 (1975).
(10) H. W. Richardson, J. R. Wasson, W. E. Hatfield, E. V. Brown, and A. Plasz, *Inorg. Chem.*, **15**, 2916 (1976).
(11) R. C. E. Belford, D. E. Fenton, and M. R. Truter, *J. Chem. Soc., Dalton Trans.*, 2208 (1972).
(12) C and H analyzed by Integral Microanalytical Labs, Raleigh, N. C.
(13) G. Guerrin, M. V. Sheldon, and C. N. Reilley, *Chemist-Analyst*, **49**, 36 (1960).
(14) Y. Hamada and I. Takeuchi, *Chem. Pharm. Bull.*, **19**, 1857 (1971).
(15) S. Foner, *Rev. Sci. Instrum.*, **30**, 548 (1959).
(16) B. N. Figgis and R. S. Nyholm, *J. Chem. Soc.*, 4190 (1958).
(17) H. St. Rade, *J. Phys. Chem.*, **77**, 424 (1973).
(18) F. R. McKim and W. P. Wolf, *J. Sci. Instrum.*, **34**, 64 (1957).
(19) D. B. Losee and W. E. Hatfield, *Phys. Rev. B*, **10**, 212 (1974).
(20) Type TG-100 FPA (Special), No. 4277, Lake Shore Cryotronics, Eden, N.Y.
(21) E. Konig, "Magnetic Properties of Transition Metal Compounds", Springer-Verlag, Berlin, 1966.
(22) I. Bernal and P. H. Rieger, *Inorg. Chem.*, **2**, 256 (1963); D. H. Chen and G. R. Luckhurst, *Trans. Faraday Soc.*, **65**, 656 (1969).
(23) J. R. Wasson, *Chemist-Analyst*, **56**, 36 (1967).
(24) J. S. Smart, "Effective Field Theories of Magnetism", W. B. Saunders, Philadelphia, Pa., 1966.
(25) P. Weiss, *Radium (Paris)*, **4**, 661 (1907).
(26) A. Santoro, A. D. Mighell, and C. W. Reimann, *Acta Crystallogr., Sect. B*, **26**, 979 (1970).
(27) G. F. Kokoszka and C. W. Reimann, *J. Inorg. Nucl. Chem.*, **32**, 3229 (1970).
(28) M. Hackmeyer and J. L. Whitten, *J. Chem. Phys.*, **54**, 3739 (1971).
(29) J. Pradilla-Sorzano and J. P. Fackler, Jr., *Inorg. Chem.*, **12**, 1174 (1973).

Contribution from the Department of Chemistry, Oklahoma State University, Stillwater, Oklahoma 74074

Coordination of Water in Alkali Metal Oxy Anion Glasses

G. Ritzhaupt and J. P. Devlin*

Received August 25, 1976 AIC60629K

There is considerable interest in the nature of the interactions experienced by water molecules within a molten salt like environment with a particular concern for the relative importance of cation–H_2O and anion–H_2O interactions.[1] Part of this interest arises because the H_2O molecule environment, which is undoubtedly quite varied in more dilute water solutions, is presumed to be more uniform since there is little chance for H_2O–H_2O interactions to further complicate the structure. However, the observation and interpretation of vibrational spectra for H_2O molecules isolated in such an environment presents some special problems, with the result that no infrared data are available for single-salt systems. In addition to the naturally great bandwidth for the H_2O stretching modes, thermal band broadening is a complicating factor at molten salt temperatures. Other discouraging factors include corrosion of cell materials, sample instability, the need for a constant appropriate H_2O vapor pressure, and the possibility of some aggregation of the H_2O molecules.

Much of the difficulty in obtaining the infrared spectra of polar molecules, such as H_2O, isolated from one another within a molten salt like environment can be avoided by isolating the molecules in a glassy salt matrix prepared by condensing the molten salt vapors at 80 K.[2] When the salt vapors are generated within a Knudsen effusion cell at temperatures near the melting point, there is no significant contamination of the glassy deposit by decomposition products for the alkali metal nitrates,[3] chlorates,[4,5] perchlorates,[6] or thiocyanates, with the exception of the lithium salt of the chlorate ion.[4]

In the present study the H_2O impurity molecules in the glassy salt matrices originated from residual water within the molten salts and/or the vacuum system after the salts were dried for 12 h at ~200 °C.[4] Thus, the precise H_2O concentrations were not known, but in each instance the ν_3

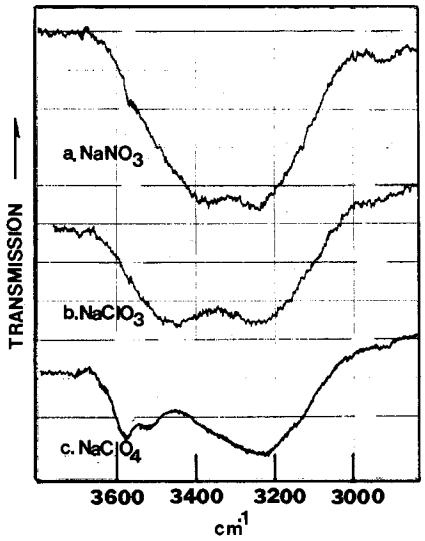

Figure 1. Infrared curves in the O–H stretching region for dilute H_2O-in-glassy-salt films at 80 K. The salts for the various curves are (a) $NaNO_3$, (b) $NaClO_3$, and (c) $NaClO_4$.

asymmetric XO_n^- stretching mode showed an optical density between 1 and 3 while that for H_2O was ~0.08 for the ν_3 mode. Therefore, since the curves for each salt were unique and highly reproducible, it is likely that the H_2O molecules were largely isolated in the glassy salt matrices. Other molecular species can be deliberately doped into the salt deposits at a desired level, but H_2O is so ubiquitous that such control is nearly impossible.

We have observed the ν_2 (bending) and the 3-μ stretching-mode infrared curves for highly dilute samples of H_2O in a variety of $M^+XO_n^-$ glasses and the results seem quite revealing. Thus, the curves in Figure 1 show the effect on the H_2O stretching-mode absorptions produced by changing the salt oxy anion while holding the cation fixed (Na^+). Each spectrum divides into two parts: a broad band near 3250 cm^{-1} which is anion insensitive and a structured band system, resembling that reported by Turnbull for a molten nitrite–nitrate mixture,[1a] which is anion sensitive and, thus, ranges in position from 3360 to 3590 cm^{-1}.

The effect of varying the cation while retaining the same anion (ClO_4^-) is shown in Figure 2. The cation effect is smaller than for the anion but is, nevertheless, definite for the high-frequency O–H stretching absorption which shifts from ~3590 cm^{-1} for $KClO_4$ to ~3530 cm^{-1} for $LiClO_4$. Although the low-frequency component is cation insensitive, a definite shoulder does appear at ~3350 cm^{-1} for the potassium salt. The top curve of Figure 2 shows that, upon crystallizing, the broad 3250-cm^{-1} band vanishes while the high-frequency O–H bands sharpen but shift very little.

The ν_2 band position was constant, within experimental error, with variation of the cation in the salt, but assumed values of 1630 ± 5, 1640 ± 5, and 1650 ± 5 cm^{-1} for the perchlorates, chlorates, and nitrates, respectively. As for the data from the O–H stretching region (Figure 1), the chlorate behavior was intermediate to that of the other two anions. The vibrational frequencies observed for H_2O molecules isolated in the glassy salt matrices are summarized in Table I.

These various results, like those from related liquid-phase studies,[1a,b,d] can be understood from a quasi-lattice view of these systems,[7] in which most of the H_2O molecules are presumed to be tightly bound through the oxygen atom in the inner coordination shell of a metal cation. Such water molecules are either weakly or non hydrogen bonded so the O–H bond remains relatively strong as reflected in the high stretching frequencies. On the other hand, the H_2O molecules

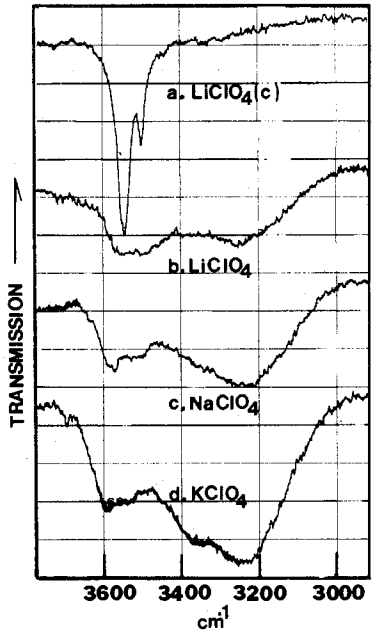

Figure 2. Infrared curves in the O–H stretching region for dilute H_2O-in-glassy-salt films (curves b–d) and H_2O in crystalline $LiClO_4$ (curve a). The salts for the glass spectra are (b) $LiClO_4$, (c) $NaClO_4$, and (d) $KClO_4$.

Table I. Vibrational Frequencies (cm^{-1}) for H_2O Molecules Isolated in Glassy Salt Matrices at 80 K

Assignment	$LiClO_4$	$NaClO_4$	$KClO_4$	$NaClO_3$	$NaNO_3$
ν_{asym} (innershell)	3550	3570	3590	3450	3360
ν_{sym} (innershell)	3490	3510	3540		
ν_2 (innershell)	1630	1630	1630	1640	1650
ν (outershell)	3250	3230	3240	3250	3240

which remain in the outer coordination shell can orient to form more normal hydrogen bonds with neighboring oxy anions and, thus, give rise to the absorption band near 3250 cm^{-1} which is both cation and anion insensitive. In applying this view to the present data, however, it should be remembered that (a) the glass system is not at equilibrium, (b) H-bonding and, thus, lower stretching frequencies are favored by the low glass temperatures, and (c) the H-bonded molecules have a much greater absorption coefficient than do the metal-coordinated H_2O molecules so the relative intensities in Figures 1 and 2 are misleading. If a ratio of 10 is taken for the absorption coefficients,[8] it follows that most of the H_2O is in the inner cation coordination shell. This is consistent with the quasi-lattice equilibrium theory and also explains our failure to observe more than a single ν_2 band in each case (i.e., that of M^+-coordinated H_2O).

The shift of this ν_2 feature to higher frequencies through the series ClO_4^-, ClO_3^-, and NO_3^- must reflect the increasing ability of the metal-coordinated H_2O molecules to hydrogen bond with the latter anions in this series. This is supported by the data of Figure 1 that indicate this interaction of metal-coordinated H_2O molecules with neighboring anions increases greatly when ClO_4^- is replaced by ClO_3^- and becomes more nearly equivalent to a normal H bond in the nitrate salt. That is, the 3360-cm^{-1} value for the high-frequency O–H band in the $NaNO_3$ glass leaves no doubt that the NO_3^- ion can H-bond, even with an M^+-coordinated H_2O molecule. By contrast, the 3590-cm^{-1} value for M^+-coordinated H_2O in $KClO_4$ approaches the "free" O–H frequency[9] and reflects the weakness of the interaction between ClO_4^- and metal-coordinated H_2O.

In an extension of this viewpoint, the data of Figure 2 suggest that the H_2O molecule enters the cation coordination

shell more efficiently for the smaller cations, as the 3250-cm^{-1} band, for the outer-shell H_2O molecules, becomes relatively more intense through the series Li^+, Na^+, and K^+. Also, the downshift in the non-H-bonded mode from 3590 cm^{-1} for $KClO_4$ to 3530 cm^{-1} for $LiClO_4$ suggests an enhanced ability of the H_2O, attached to the smaller cations, to interact with neighboring ClO_4^- ions.

Acknowledgment. This research has been sponsored by the National Science Foundation.

Registry No. H_2O, 7732-18-5; $LiClO_4$, 7791-03-9; $NaClO_4$, 7601-89-0; $KClO_4$, 7778-74-7; $NaClO_3$, 7775-09-9; $NaNO_3$, 7631-99-4.

References and Notes

(1) See for example (a) A. G. Turnbull, *Aust. J. Chem.*, **24**, 2213 (1974); (b) K. Balasubrahmanyam and G. J. Janz, *J. Soln. Chem.*, **1**, 445 (1972); (c) B. G. Oliver and G. J. Janz, *J. Phys. Chem.*, **75**, 2948 (1971); (d) M. Strauss and M. C. R. Symons, *Chem. Phys. Lett.*, **39**, 471 (1976); (e) D. E. Irish, *Ionic Interact.*, **2**, 187 (1971).
(2) G. Pollard, N. Smyrl, and J. P. Devlin, *J. Phys. Chem.*, **76**, 1826 (1972).
(3) D. Smith, D. W. James, and J. P. Devlin, *J. Chem. Phys.*, **54**, 4437 (1971).
(4) N. Smyrl and J. P. Devlin, *J. Chem. Phys.*, **60**, 2540 (1974).
(5) A. Büchler, D. J. Meschi, P. Mohazzabi, and W. A. Searcy, *J. Chem. Phys.*, **64**, 4800 (1976).
(6) G. Ritzhaupt and J. P. Devlin, *J. Phys. Chem.*, **79**, 2265 (1975).
(7) J. Braunstein, *J. Phys. Chem.*, **71**, 3402 (1967).
(8) G. C. Pimentel and A. L. McClellan, "The Hydrogen Bond", W. H. Freeman, San Francisco, Calif., 1960, p 101.
(9) G. E. Walrafen, *J. Chem. Phys.*, **48**, 244 (1968).

Contribution from the Department of Chemistry, University of Minnesota, Minneapolis, Minnesota 55455

Synthesis and Characterization of a New Seven-Coordinate Ruthenium(IV) Complex. Crystal and Molecular Structure of Iodotris(*N,N*-dimethyldithiocarbamato)ruthenium(IV)–Iodine

B. M. Mattson and L. H. Pignolet*

Received September 20, 1976 AIC60690P

The reaction of iodine with various bis- and tris(*N,N*-disubstituted-dithiocarbamato)metal complexes, $M(R_2dtc)_n$, n = 2 or 3, has been shown to form stable complexes in which the metal is in an unusually high oxidation state. Included among these are $[Ni(Bu_2dtc)_3]I_n$, n = 1 or 3 (Bu = *n*-butyl),[1,2] $[M(Bu_2dtc)_3]I_3$, M = Pd or Pt,[3] $[Cu(Bu_2dtc)_2]$,[2,4] and *cis*-$Pt(Bu_2dtc)_2I_2$.[3] In all but the last example the iodine functions as a counteranion, I^- or I_3^-. *cis*-$Pt(Bu_2dtc)_2I_2$ has been characterized by x-ray analysis[3] and is synthesized initially in the trans stereochemistry by an interesting solid-state reaction between $Pt(Bu_2dtc)_2$ and I_2. The compound rapidly converts into the cis form in solution.[3]

In this note we report the reaction between iodine and $M(R_2dtc)_3$ complexes where M = iron and ruthenium in CH_2Cl_2 solution. A rapid reaction occurs with complexes of both metals yielding pure crystalline compounds. In the case of ruthenium a diamagnetic complex is formed with stoichiometry $Ru(R_2dtc)_3I_3$ for R_2 = Me_2, Et_2, Bzl_2, and (Me)(Ph) (Me = methyl, Et = ethyl, Bzl = benzyl, Ph = phenyl). An x-ray analysis for R_2 = Me_2 shows the molecule to be seven-coordinate and to have a distorted pentagonal-bipyramidal geometry with two R_2dtc ligands spanning equatorial sites and the third spanning axial and equatorial sites. One iodine atom is covalently coordinated to the ruthenium atom in an axial position while an I_2 molecule strongly solvates the iodine atom. The compound is structurally similar to three other d^4 metal complexes, $Ru(Et_2dtc)_3Cl$,[5] $Mo(Bu_2dtc)_3NO$,[6] and $Re(Et_2dtc)_3CO$.[7] The x-ray analysis was carried out in order to account for unusual ^1H NMR properties (vide infra) and to elucidate the nature of the iodine atoms and the geometry of the coordination core. The analogous reaction with the iron complex (R_2 = Me_2) yielded a paramagnetic compound which is identified to be $Fe(Me_2dtc)_2I$.[8] Details of the characterization of these complexes and the x-ray structure of $Ru(Me_2dtc)_3I\cdot I_2$ are reported in this note.

Experimental Section

Spectra. ^1H NMR spectra were recorded using a Varian XL-100-15 spectrometer equipped with a variable-temperature probe. IR spectra were recorded in KBr disks with a Perkin-Elmer Model 237 grating spectrophotometer. Electronic absorption spectra were obtained in CH_2Cl_2 solution at 25 °C with a Cary Model 14 spectrophotometer. Magnetic susceptibilities were determined by the Faraday method at 25 °C using $Hg[Co(SCN)_4]$ as calibrant.

Conductivity experiments were carried out using a Yellow Springs Instrument Co. Model 31 conductivity bridge. Reagent grade nitromethane was purified by double distillation from anhydrous $CaCl_2$ onto anhydrous $CaSO_4$ under nitrogen and Spectrograde 1,2-dichloroethane was used without purification.

Preparation of Compounds. $Ru(R_2dtc)_3I_3$. $Ru(Me_2dtc)_3$, 0.5 g purified by column chromatography,[9] was dissolved in ca. 300 ml of CH_2Cl_2 and then filtered. I_2 (0.4 g) was dissolved in CH_2Cl_2 and added to the solution of $Ru(Me_2dtc)_3$ affording metallic gold crystals of $Ru(Me_2dtc)_3I_3$. Recrystallization was achieved by continuous Soxhlet extraction using CH_2Cl_2. Anal. Calcd for $RuC_9H_{18}N_3S_6I_3$: C, 12.83; H, 2.15. Found: C, 13.09; H, 2.21. Electronic absorption spectrum (λ_{max} (nm), log ϵ): 265, 4.59; 289, 4.60; 356, 4.34; 460 sh, 3.58. IR spectrum (cm^{-1}) (ν_{C-N} 1548, 1537): 1391, 1249, 1151. ^1H NMR (CD_2Cl_2): τ 6.91 (singlet). Mp 218 °C dec; conductivity (8.31 × 10^{-4} M in nitromethane at 25 °C) Λ = 77 Ω^{-1} cm^2 mol^{-1}. Analogous complexes with R_2 = Et_2, Bzl_2, and (Me)(Ph) were prepared in an identical manner except that purification was achieved by recrystallization from CH_2Cl_2–heptane solution. Complete characterization data for these compounds are listed in supplementary Table SI.

$Fe(Me_2dtc)_2I$ was prepared in a manner identical manner with that for $Ru(R_2dtc)_3I_3$, and purification was achieved by Soxhlet extraction from CH_2Cl_2. Anal. Calcd for $FeC_6H_{12}N_2S_4I$: C, 17.03; H, 2.86; N, 6.62; I, 29.99. Found: C, 17.07; H, 2.91; N, 6.53; I, 30.19. Electronic absorption spectrum (λ_{max} (nm), log ϵ): 305, 4.29; 377, 4.10; 456, 3.93; 500 sh, 3.78; 604, 3.66. IR spectrum (cm^{-1}) ($\nu_{C\cdots N}$ 1550): 1391, 1239, 1151, 922. Mp 307 °C dec; magnetic susceptibility χ_m^{cor} = 700 × 10^{-5} cgsu/mol at 25 °C; μ_{eff} = 4.09 μ_B.

Structure Determination. The quality of the crystals was poor so that much difficulty was encountered in finding a suitable one. We proceeded with a small flat needle-shaped crystal of dimensions 0.28 mm × 0.12 mm × 0.04 mm. The monoclinic crystal was mounted with the *a* axis parallel to the spindle axis. The cell constants, a = 6.261 (6) Å, b = 17.178 (10) Å, c = 10.986 (7) Å, β = 103.83 (5)°, and V = 1147 Å^3, were determined by a least-squares refinement using θ-angle values for 10 Mo Kα peaks carefully centered on the diffractometer. The measured density, 2.40 g/cm^3, agrees with the calculated density, 2.44 g/cm^3, for Z = 2. Systematic extinctions, ($0k0$, $k \neq 2n$), indicated the space group to be $P2_1$ or $P2_1/m$. The latter was confirmed by the solution of the structure. Since Z = 2, this requires that individual molecules contain either a mirror plane or a center of symmetry.

Intensity data were collected on a four-circle Hilger and Watts automatic diffractometer using Zr-filtered Mo Kα radiation. Of the 1702 independent reflections collected out to θ = 26°, 1257 with $F_o^2 > 2\sigma(F_o^2)$ were used in solution and refinement of the structure. Two standard reflection intensities were checked at intervals of 20 sequential reflections and no changes greater than 4% from the average value and no trends with time were noted.

The data were processed in the manner described by Corfield, Doedens, and Ibers,[10] using 0.03 for p in the $\sigma(I)$ equation. The intensity data were corrected for Lorentz and polarization effects as well as for absorption (μ = 52.7 cm^{-1}). Conventional heavy-atom techniques were used to solve the structure, and refinement,[11] with all nonhydrogen atoms thermally anisotropic by full-matrix least-squares methods, converged R and r to their final values of 0.078 and 0.027, respectively.[12] In the final difference Fourier, the highest peak